Colloids with key-lock interactions: Nonexponential relaxation, aging, and anomalous diffusion

Nicholas A. Licata and Alexei V. Tkachenko

Department of Physics and Michigan Center for Theoretical Physics, University of Michigan,
450 Church Street, Ann Arbor, Michigan 48109, USA

The dynamics of particles interacting by key-lock binding of attached biomolecules are studied theoretically. Experimental realizations of such systems include colloids grafted with complementary single-stranded DNA (ssDNA), and particles grafted with antibodies to cell-membrane proteins. Depending on the coverage of the functional groups, we predict two distinct regimes. In the low coverage *localized regime*, there is an exponential distribution of departure times. As the coverage is increased the system enters a *diffusive regime* resulting from the interplay of particle desorption and diffusion. This interplay leads to much longer bound state lifetimes, a phenomenon qualitatively similar to *aging* in glassy systems. The diffusion behavior is analogous to dispersive transport in disordered semiconductors: depending on the interaction parameters it may range from a finite renormalization of the diffusion coefficient to anomalous, *subdiffusive* behavior. We make connections to recent experiments and discuss the implications for future studies.

I. INTRODUCTION

In this paper we present a theoretical study of desorption and diffusion of particles which interact through key-lock binding of attached biomolecules. It is becoming common practice to functionalize colloidal particles with single-stranded DNA (ssDNA) to achieve specific, controllable interactions [1–6]. Beyond the conceptual interest as a model system to study glassiness [7] and crystallization, there are a number of practical applications. Colloidal self-assembly may provide a fabrication technique for photonic band gap materials [8,9]. One of the major experimental goals in this line of research is the self-assembly of colloidal crystals using DNA mediated interactions. The difficulty stems in part from the slow relaxation dynamics in these systems. The main goal of this paper is to understand how the collective character of key-lock binding influences the particle dynamics. In doing so we gain valuable insight into the relaxation dynamics, and propose a modified experimental setup whose fast relaxation should facilitate colloidal crystallization.

Similar systems have also attracted substantial attention in other areas of nanoscience. In particular, by functionalizing nanoparticles with antibodies to a particular protein, the nanoparticles have potential applications as smart, cell-specific drug delivery vehicles [10,11]. These nanodevices take advantage of the fact that certain cancerous cells over-express cell membrane proteins, for example, the folate receptor. An improved understanding of desorption and diffusion on the cell membrane surface may have implications for optimizing the design of these drug delivery vehicles.

In what follows we present our results on the dynamics of particles which interact through reversible key-lock binding. The plan for the paper is the following. In Sec. II we introduce the key-lock model and explain the origin of the two model parameters Δ and $\bar{m}$. The parameter Δ determines the binding energy for the formation of a key-lock pair. The parameter $\bar{m}$ is the mean of the distribution for the number of key-lock bridges. Depending on $\bar{m}$, which is related to the coverage of the functional groups (e.g., ssDNA), there are

two distinct regimes. At low coverage there is an exponential distribution of departure times, but no true lateral diffusion. As the coverage increases, we enter a regime where the particle dynamics is a result of the interplay between desorption and diffusion. An estimate is provided for the value of $\bar{m}$ which determines the crossover from the localized to the diffusive regime. In Sec. III the localized regime is discussed in detail. In this regime the particle is attached to a finite cluster and remains localized near its original location until departing. We derive the partition function for the finite clusters, and calculate the departure time distribution. In Sec. IV we determine the departure time distribution in the diffusive regime. We present an effective Arrhenius approximation for the hopping process and a Fourier transform method which greatly simplifies the calculation. In Sec. V we discuss the random walk statistics for the particles' in-plane diffusion. A set of parametric equations is derived to relate the average diffusion time to the mean squared displacement. The lateral motion is analogous to dispersive transport in disordered semiconductors, ranging from standard diffusion with a renormalized diffusion coefficient to anomalous, subdiffusive behavior. In Sec. VI we connect our results to recent experiments with DNA-grafted colloids. We then discuss the implications of the work for designing an experiment which facilitates faster colloidal crystallization. In Sec. VII we conclude by summarizing our main results.

II. MODEL

We now present the model, where a single particle interacts with a flat two-dimensional surface by multiple key lock binding (see Fig. 1). At each location on the surface there are m key-lock bridges which may be open or closed, with a binding energy of ϵ for each key-lock pair. Here we have neglected the variation in ϵ. In the case of the DNA-colloidal system mentioned in the Introduction, the model parameter ϵ is related to the hybridization free energy of the DNA. The resulting m-bridge free energy plays the role of an effective local potential for the particle [12]:
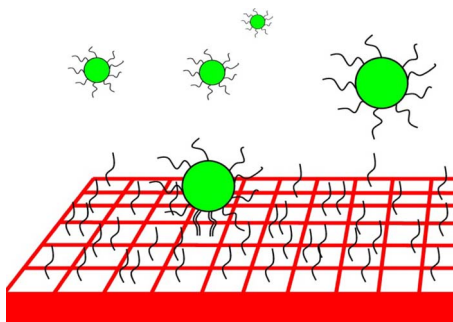
FIG. 1. (Color online) Graphical depiction of particles interacting with a flat, 2D substrate by multiple key-lock binding.

$$U(m) = -k_B T m \Delta, \tag{1}$$

$$\Delta \equiv \ln(1 + \exp[\epsilon/k_B T]). \tag{2}$$

Generically, m is a Poisson distributed random number $P_m = \bar{m}^m \exp(-\bar{m})/m!$ where $\bar{m}$ denotes the mean of the distribution. The model parameter $\bar{m}$ is a collective property of the particle-surface system. For example, consider the case of dendrimers functionalized with folic acid, which can be utilized for targeted, cell specific chemotherapy. The folic acid on the dendrimer branch ends form key-lock bridges with folate receptors in the cell membrane. In this case $\bar{m}$ will depend on the distribution of keys (folic acids) on the dendrimer, and the surface coverage of locks (folate receptors) in the cell membrane.

At each location, the particle is attached to the surface by m bridges. To detach from the surface the particle must break all its connections, in which case it departs and diffuses away into solution. Alternatively the particle can hop a distance a to a new location characterized by a new value of the bridge number m. By introducing the correlation length a, we have coarse-grained the particle motion by the distance after which the new value of the bridge number becomes statistically independent of the value at the previous location. In the localized regime the particle remains close to its original location until departing. In the diffusive regime the particle is able to fully explore the surface through a random walk by multiple breaking and reforming of bridges.

Naively one might expect the crossover between the two regimes to occur at the percolation threshold, where one first encounters an infinitely connected cluster of sites with $m > 0$. However, the crossover from the localized to diffusive regime occurs at smaller $\bar{m}$ than predicted by percolation theory. If $p_c = 1/2$ denotes the critical probability for site percolation on the triangular lattice, the percolation transition occurs at $\bar{m} = \ln(2)$. There are two alternative estimates for the crossover from the localized to the diffusive regime. The first is to compare the average number of steps $n = \exp(\Delta \bar{m})$ the particle takes before departing (see Sec. IV) to the characteristic cluster size $s_c = 1/\ln(1/\lambda p)$ below the percolation threshold. Here $\lambda = 5.19$ is a numerical constant for the triangular lattice [13], and in the percolation language $p = 1 - \exp(-\bar{m})$ is the occupancy probability. The crossover condition $n = s_c$ can be expressed as a function of $\bar{m}$,
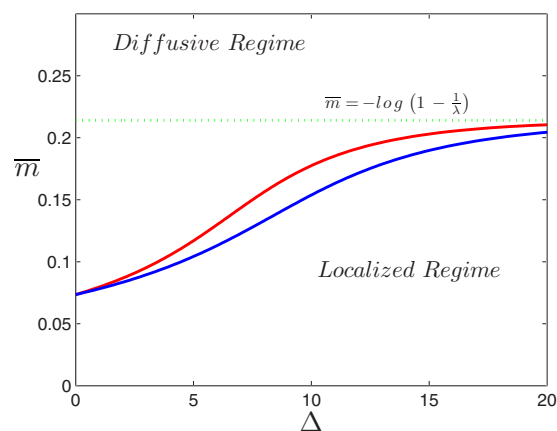

FIG. 2. (Color online) The crossover from the localized to the diffusive regime below the percolation threshold. Estimates based on the characteristic cluster size [Eq. (3), dashed line] and confinement of the random walk [Eq. (4), solid line] give similar crossovers. For large Δ the crossover condition is $\bar{m} = -\ln(1 - \frac{1}{\lambda})$.

$$\Delta = -\frac{1}{\bar{m}} \ln\{-\ln[\lambda(1 - e^{-\bar{m}})]\}. \tag{3}$$

Alternatively, in the localized regime the particles' random walk is confined by the characteristic cluster size. Below percolation the radius of gyration of the cluster is $R_s \sim s^\rho$ with $\rho = 0.641$ in two dimensions. Comparing the radius of gyration of the cluster to the radius of gyration for the particles' random walk, the crossover occurs at $n = (s_c)^{2\rho}$,

$$\Delta = -\frac{2\rho}{\bar{m}} \ln\{-\ln[\lambda(1 - e^{-\bar{m}})]\}. \tag{4}$$

Since 2ρ differs from 1 by less than 30%, both conditions give similar crossovers (see Fig. 2). The saturation at $\bar{m} = -\ln(1 - \frac{1}{\lambda})$ occurs for very large Δ, as a result for binding energies of a few $k_B T$ per bridge the crossover occurs at $\bar{m} \simeq 0.1$.

III. LOCALIZED REGIME

In the percolation language, when the occupancy probability $p = 1 - \exp(-\bar{m})$ is small, particles are localized on finite clusters. In this localized regime particles are able to fully explore the cluster to which they are attached before departing. This thermalization of particles with finite clusters permits an equilibrium calculation of the cluster free energy $F = -k_B T \ln\langle Z \rangle$. The departure rate is given by the Arrhenius relation $K = \frac{1}{\tau_0} \exp(F/k_B T)$. Here τ_0 is a characteristic time scale for bridge formation. The probability that the particle departs between t and $t + dt$ is determined from the departure time distribution $\Phi(t)dt \simeq K \exp[-Kt]dt$.

To begin we calculate the partition function for the finite clusters. The cluster is defined as s connected sites on the lattice, all of which are characterized by $0 < m < m^*$ bridges. For Poisson distributed bridge numbers the partition function for the finite cluster is

$$Z(m^*,s) = \sum_{i=1}^{s} \sum_{m_i=1}^{m^*-1} \widetilde{P}_{m_i} \exp(\Delta m_i)$$

$$= \frac{s}{\exp(\bar{m}) - 1}[\exp(\bar{m}e^\Delta)Q(\bar{m}e^\Delta,m^*) - 1]. \quad (5)$$

Because by definition the cluster does not contain sites with $m = 0$ bridges we have renormalized the probability distribution $\widetilde{P}_m = P_m/[1 - \exp(-\bar{m})]$ so that $\sum_{m=1}^{\infty}\widetilde{P}_m = 1$. Here $Q(x,m^*) \equiv \Gamma(x,m^*)/\Gamma(m^*) = \exp(-x)\sum_{k=0}^{m^*-1}x^k/k!$ is the regularized upper incomplete Γ function. In the language of the statistics of extreme events, $m^* - 1$ is the maximum "expected" value of m in a sample of s independent realizations [14]. The point is that on finite clusters we should not expect to achieve arbitrarily large values of the bridge number. Hence when averaging the partition function to obtain the cluster free energy one should only average over sites with $m < m^*$. The distribution function for m^* is obtained by noting that the probability that all s values of m are less than m^* is $(\sum_{m=1}^{m^*-1}\widetilde{P}_m)^s = \left(\frac{\exp(\bar{m})Q(\bar{m},m^*)-1}{\exp(\bar{m})-1}\right)^s$. By differentiating this quantity with respect to m^* we obtain the distribution function for the maximum expected value of m,

$$f_s(m^*) = s\left(\frac{\exp(\bar{m})Q(\bar{m},m^*) - 1}{\exp(\bar{m}) - 1}\right)^{s-1}\widetilde{P}_{m^*}. \quad (6)$$

The cluster size distribution below the percolation threshold is exponential [15] with characteristic cluster size $s_c = 1/\ln(1/\lambda p)$,

$$p_s(p) = \frac{1 - \lambda p}{\lambda}\exp\left(-\frac{s}{s_c}\right). \quad (7)$$

The summation over s can be performed analytically, which allows the result to be expressed as a single summation over m^*,

$$\langle Z \rangle = \sum_{m^*=2}^{\infty}\sum_{s=1}^{\infty} p_s(p)f_s(m^*)Z(m^*,s) = \frac{\lambda\{1 - \lambda[1 - \exp(-\bar{m})]\}}{\exp(\bar{m}) - 1}$$

$$\times \sum_{m^*=2}^{\infty}\widetilde{P}_{m^*}[\exp(\bar{m}e^\Delta)Q(\bar{m}e^\Delta,m^*) - 1]\frac{1 + y(m^*)}{[1 - y(m^*)]^3}, \quad (8)$$

$$y(m^*) = \lambda[Q(\bar{m},m^*) - \exp(-\bar{m})]. \quad (9)$$

For fixed $\bar{m}$, as in the plot (see Fig. 3), changing Δ is directly related to a change in the average binding free energy. Increasing Δ leads to a reduction in the rate of particle departure.

IV. DIFFUSIVE REGIME

The departure time distribution changes significantly in the diffusive regime. In this regime the particle can explore the surface to find a more favorable connection site, which leads to a longer lifetime for the bound state. This phenomenon is qualitatively similar to *aging* in glassy systems. In these systems one finds that the response to an external field
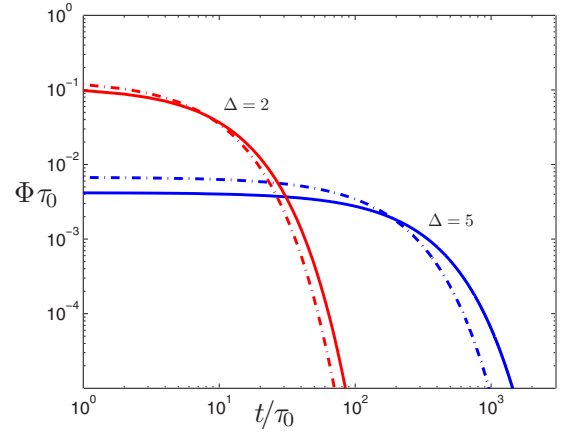

FIG. 3. (Color online) Departure time distribution function vs time in the localized regime with $\bar{m} = 0.1$. The results of our calculation (solid lines) are compared to single exponential relaxation with departure rate $K = \frac{\exp(-\Delta)}{\tau_0}$ (dotted lines).

is time dependent [16]. In the magnetic analogy this leads to a time dependence of the magnetization. Below the glass temperature, the longer one waits before applying the external magnetic field, the more time the system has to settle into deep energy wells, and the smaller the response. In our case, the diffusive exploration of the particle allows it to find a deeper energy well, which leads to an increase in the bound state lifetime.

As a result, the departure time distribution must now reflect not only desorption, but also hopping to adjacent sites. The hopping rate between neighboring sites i and j is given by an Arrhenius law $\kappa_{i\to j} = \frac{1}{\tau_0}\exp[-\Delta(m_i - m_j)\theta(m_i - m_j)]$, with $\theta(x)$ the Heaviside step function. In a lattice model with coordination number z the dwell time τ_m at a site with m bridges is calculated by averaging over the hopping rates to the nearest neighbors (see Fig. 4),
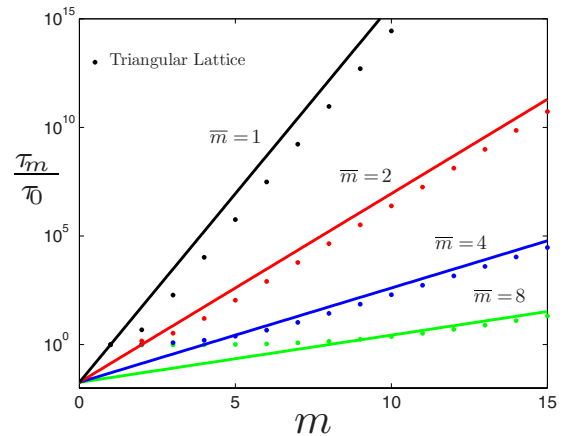

FIG. 4. (Color online) Comparison of the ensemble averaged dwell time in a lattice model [Eq. (10)] to the effective Arrhenius approximation [Eq. (11)]. In the plot the product $\Delta\bar{m} = 4$ is held constant.

$$\tau_m = \left\langle \frac{1}{\frac{1}{z}\sum_{i=1}^{z} \kappa_{m\to i}} \right\rangle_{m_1 \cdots m_z}$$

$$= z \sum_{m_1=1}^{\infty} \cdots \sum_{m_z=1}^{\infty} \widetilde{P}_{m_1} \cdots \widetilde{P}_{m_z} \frac{1}{\sum_{i=1}^{z} \kappa_{m\to i}}. \qquad (10)$$

Fortunately, this ensemble averaging procedure can be accurately approximated by an effective Arrhenius relation:

$$\tau_m = \tau_0 \exp[\Delta(m - \bar{m})]. \qquad (11)$$

The validity of the approximation is most important for sites with $m \geq \bar{m}$ bridges, since the diffusive exploration allows the particle to quickly cascade into these deep energy wells.

The effective Arrhenius relation greatly simplifies the calculation, since so long as $\Delta\bar{m}$ is sufficiently large, the probability of the particle still being attached to the surface after an n step random walk is $(1 - K_m\tau_m)^{n-1} = [1 - \exp(-\Delta m)]^{n-1}$. Here $K_m = \frac{1}{\tau_0}\exp(-\Delta m)$ is the departure rate from a site with m bridges. Interestingly, in this approximation scheme the attachment probability is independent of the particular bridge numbers $\{m_1, \ldots, m_n\}$ realized during the walk. Thus the probability of departure f_n after exactly n steps is

$$f_n = [\exp(\gamma) - 1]\exp(-\gamma n), \qquad (12)$$

$$\gamma \equiv -\ln[1 - \exp(-\Delta\bar{m})]. \qquad (13)$$

The average number of steps for the random walk is $\sum_{n=1}^{\infty} n f_n = \exp(\Delta\bar{m})$. To calculate the departure time distribution $\Phi(t)$ we use f_n to average over the departure time distribution for walks with a given n, $\phi_n(t)$,

$$\Phi(t) = \sum_{n=1}^{\infty} f_n \phi_n(t), \qquad (14)$$

$$\phi_n(t) = \prod_{j=1}^{n}\left[\sum_{m_j=1}^{\infty} \widetilde{P}_{m_j} \int_0^{\infty} dt_j \left(\frac{-dS_{m_j}(t_j)}{dt_j}\right)\right]\delta\left(t - \sum_{k=1}^{n} t_k\right). \qquad (15)$$

Here $S_m(t)$ is the survival probability at time t for a site with m bridges, used to determine the probability of departure between t and $t + dt$. If there was only one hopping pathway with rate κ, we would have $-\frac{dS}{dt} = \kappa \exp(-\kappa t)$. The generalization accounts for the fact that the particle can hop to any of its z neighbors, and the probability of departure is not simply exponential,

$$S_m(t) = \left(\sum_{a=1}^{\infty} \widetilde{P}_a \exp[-t\kappa_{m\to a}]\right)^z. \qquad (16)$$

It is convenient to Fourier transform $\phi_n(t)$ so that one can sum the resulting geometric series for $\Phi(\omega)$,

$$\phi_n(\omega) = \int_{-\infty}^{\infty} \phi_n(t)\exp[-i\omega t]dt = X(\omega)^n, \qquad (17)$$

$$X(\omega) \equiv \sum_{m=1}^{\infty} \widetilde{P}_m \sum_{m_1=1}^{\infty} \cdots \sum_{m_z=1}^{\infty} \widetilde{P}_{m_1} \cdots \widetilde{P}_{m_z}\left(\frac{\sum_{i=1}^{z}\kappa_{m\to m_i}}{z}\cdot\frac{1}{\sum_{i=1}^{z}\kappa_{m\to m_i} + i\omega}\right), \qquad (18)$$

$$\Phi(\omega) = [\exp(\gamma) - 1]\sum_{n=1}^{\infty}[\exp(-\gamma)X(\omega)]^n$$

$$= [\exp(\gamma) - 1]\frac{X(\omega)}{\exp(\gamma) - X(\omega)}. \qquad (19)$$

To facilitate a simpler calculation, we employ a coarse-graining procedure to dispense with the tensor indices $\{m, m_1, \ldots, m_z\}$ in the definition of $X(\omega)$. In the summation there are many terms for which the value of $\sum_{i=1}^{z}\kappa_{m\to m_i}$ are equal, but with different weight factors $\widetilde{P}_m\widetilde{P}_{m_1}\cdots\widetilde{P}_{m_z}$. To eliminate this degeneracy we introduce a smooth function $f(\kappa)$ normalized according to $\int f(\kappa)d\kappa = 1$,

$$X(\omega) \simeq \int f(\kappa)\frac{\kappa}{\kappa + i\omega}d\kappa. \qquad (20)$$

The inverse Fourier transform is performed using the residue theorem to obtain the final result. The contour integral is closed in the upper half plane, with all the poles on the imaginary axis at $\omega = iz$,

$$\Phi(t) = \frac{1}{2\pi}\int_{-\infty}^{\infty}\Phi(\omega)\exp[i\omega t]d\omega$$

$$= \frac{[\exp(\gamma) - 1]}{2\pi}2\pi i\sum_{r=1}^{\infty} res_{\omega=\omega_r}\left[\frac{\exp[i\omega t]X(\omega)}{\exp(\gamma) - X(\omega)}\right]$$

$$= [\exp(\gamma) - 1]i\sum_{r=1}^{\infty} res_{\omega=\omega_r}$$

$$\times\left[\frac{\exp[i\omega_r t][X(\omega_r) + (\omega - \omega_r)(dX/d\omega)_{\omega=\omega_r} + \cdots]}{\exp(\gamma) - [X(\omega_r) + (\omega - \omega_r)(dX/d\omega)_{\omega=\omega_r} + \cdots]}\right]$$

$$= [\exp(\gamma) - 1]i\sum_{r=1}^{\infty}\left[\frac{-\exp[i\omega_r t]X(\omega_r)}{(dX/d\omega)_{\omega=\omega_r}}\right]$$

$$= \exp(\gamma)[\exp(\gamma) - 1]\sum_{r=1}^{\infty}\frac{\exp(-z_r t)}{Y(z_r)}, \qquad (21)$$

$$Y(z_r) \equiv \int f(\kappa)\frac{\kappa}{(\kappa - z_r)^2}d\kappa. \qquad (22)$$

Here z_r labels the roots of the equation,

$$\exp(\gamma) - X(iz) = 0. \qquad (23)$$

The benefit of the coarse graining is now more transparent, as the residues are all labeled by a single index r as opposed to the tensor indices $\{m, m_1, \ldots, m_z\}$.
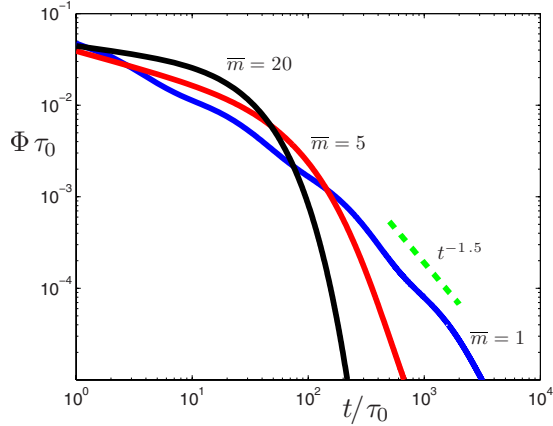
FIG. 5. (Color online) Departure time distribution function vs time as determined by Eq. (21) in the diffusive regime. In the plot the average binding energy is held constant at $3k_BT$. The theoretically determined departure time distribution can be compared to an experiment with DNA-grafted colloids (see Sec. VI) which observed power law behavior with exponent −1.5.

In Fig. 5 the departure time distribution is plotted in the diffusive regime. The optimal regime for fast particle departure is to have a large number ($\bar{m} \sim 10$) of weakly bound key-lock bridges. In this scenario the departure time distribution is accurately approximated as a single exponential, $\Phi(t) = K_{\bar{m}} \exp(-K_{\bar{m}}t)$.

V. DIFFUSION

We now turn to discuss the statistics for the in-plane diffusion of the particle. We first note that the in-plane trajectory of the particle subjected to a delta-correlated random potential remains statistically equivalent to an unbiased random walk. As a result, the mean squared displacement for an n step random walk remains $\langle r^2 \rangle = na^2$. As the particle explores the landscape it cascades into deeper energy wells, the hopping time increases, and the diffusion gets slower. In the limit $n \to \infty$ the average hopping time can be determined from the equilibrium canonical distribution. For Poisson distributed bridge numbers m, this corresponds to a finite renormalization of the diffusion coefficient D^* with $D_0 = a^2/4\tau_0$,

$$\langle t \rangle = n \langle \tau_m \rangle = n\tau_0 \exp(-\Delta\bar{m}) \sum_{m=1}^{\infty} \widetilde{P}_m \exp(\Delta m)$$

$$= n\tau_0 \frac{\exp(\bar{m}e^{\Delta}) - 1}{\exp(\Delta\bar{m})[\exp(\bar{m}) - 1]}, \quad (24)$$

$$D^* \equiv \frac{1}{4}\frac{\partial\langle r^2 \rangle}{\partial\langle t \rangle} = D_0 \frac{\exp(\Delta\bar{m})[\exp(\bar{m}) - 1]}{\exp(\bar{m}e^{\Delta}) - 1}. \quad (25)$$

This "ergodic" behavior is only achieved after a very long time. Generally, an n step random walk cannot visit sites with arbitrarily large m. In this transient regime one should only average over sites with $m < m^*$. In the language of the statistics of extreme events, $m^* - 1$ is the maximum "ex-
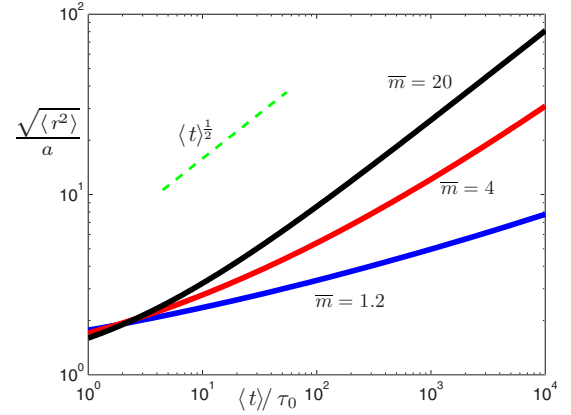

FIG. 6. (Color online) Root mean squared displacement vs time with $\Delta\bar{m} = 4$. The curves are calculated from the parametric Eqs. (26) and (27).

pected" value of m in a sample of n independent realizations [14]. Even with this complication, the average diffusion time $\langle t \rangle$ and the mean squared displacement $\langle r^2 \rangle$ can both be expressed in terms of m^*, which defines their relationship in parametric form,

$$\langle r^2 \rangle = \frac{a^2}{P(\bar{m}, m^*)}, \quad (26)$$

$$\langle t \rangle = \frac{\langle r^2 \rangle}{D^*}\left(1 - \frac{P(\bar{m}e^{\Delta}, m^*)}{1 - \exp(-\bar{m}e^{\Delta})}\right). \quad (27)$$

Here $P(x, m^*) \equiv \gamma(x, m^*)/\Gamma(m^*) = \exp(-x)\Sigma_{k=m^*}^{\infty} x^k/k!$ is the regularized lower incomplete Γ function. In the limit $m^* \to \infty$ we recover the renormalized diffusion relation $\langle t \rangle = \langle r^2 \rangle/D^*$, although this occurs at very long, often unrealistic times. In the transient regime we expect anomalous, subdiffusive behavior. As indicated in Fig. 6, this subdiffusive behavior is typical for strong enough key-lock interactions. Figure 7 is a plot of the dimensionless diffusion coefficient vs time. The anomalous diffusion may be well described by a power law $\langle r^2(t) \rangle \sim \langle t \rangle^{\alpha}$ with a nonuniversal exponent $\alpha < 1$.
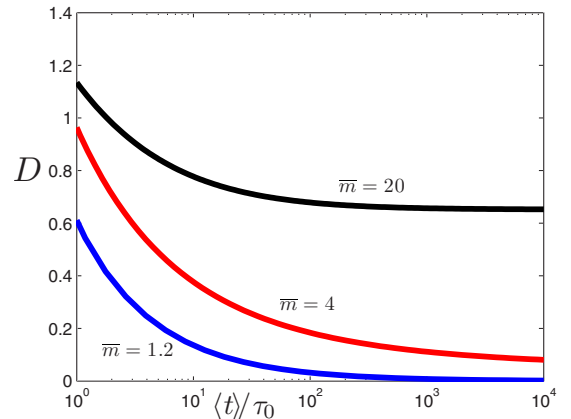

FIG. 7. (Color online) The dimensionless diffusion coefficient $D \equiv \frac{1}{4D_0}\frac{\partial\langle r^2 \rangle}{\partial\langle t \rangle}$ plotted against time.
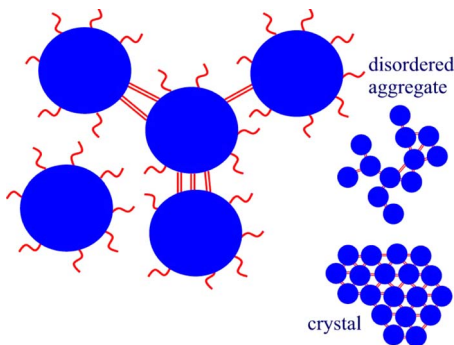
FIG. 8. (Color online) Graphical depiction of key-lock binding between nanoparticles functionalized with complementary ssDNA. The resulting structures can be disordered, fractal-like aggregates, or crystalline.

FIG. 9. (Color online) Plot of the characteristic times T_{dep} and T_{dif} vs $\bar{m}$ at constant binding energy [const=4 in Eq. (29)].

There is an analogy between our results and dispersive transport in amorphous materials. In these systems a length dependence of the effective mobility [17] can be interpreted within the context of the statistics of extreme events [14]. The time required for charge carriers to travel through the material depends on the dwell times spent at all of the trapping centers. Since this transit time will be dominated by the dwell time of the deepest trapping center, one would like to know how the thickness of the material effects the distribution for the largest trapping depth. The analogy to our result is made by replacing the material thickness with the number of steps in the random walk n, and replacing the distribution for the largest trap depth with the distribution for m^*, since the bridge number is related to energy by Eq. (1).

VI. EXPERIMENT

We now would like to make a connection between our results and recent experiments with DNA-grafted colloids. The departure time distribution can be compared to an experiment which determined the time-varying separation of two DNA-grafted colloids in an optical trap [1]. In the experimental setup, two particles are bound by DNA bridges, and after breaking all connections diffuse to the width of the optical trap. Because the length of the DNA chains grafted on the particle is much shorter than the particle radius, surface curvature effects can be neglected. The interaction resembles that of a particle interacting with a patch on a two-dimensional substrate. Experimentally the tail of the departure time distribution was observed to be a power law $\Phi(t) \sim t^{-1.5}$. Qualitatively similar behavior is predicted by the theory with $\bar{m} \sim 1$ and average binding free energy of several $k_B T$ (see $\bar{m}=1$ curve in Fig. 5).

In addition, our work provides insight into the slow crystallization dynamics of key-lock binding particles (see Fig. 8). In [2], 1-μm diameter particles grafted with ssDNA formed reversible, disordered aggregates. The average number of key-lock bridges between particles was $\bar{m} \sim 2$. The authors of [1] observed random hexagonal close packed crystals by further reducing the surface density of DNA strands on 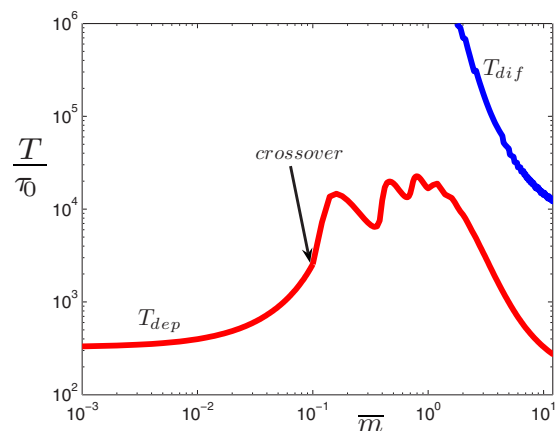the particles. The crystallization process requires that particles rapidly detach and reattach at the desired lattice location. In the localized regime particle desorption is the relevant process.

In the diffusive regime surface diffusion also plays a role in the rearrangement of particles into the desired crystalline structure. To determine which process is more important for particle rearrangement, we can compare the departure time with the time required for a particle to diffusively explore the surface of a particle to which it is bound. The time T_{dep} required for 90% of the particles to depart is

$$0.1 = \int_{T_{dep}}^{\infty} \Phi(t) dt. \tag{28}$$

To estimate the time required for diffusive rearrangement T_{dif} we use the parametric Eqs. (26) and (27). In [2] particles of radius $R=0.5$ μm were grafted with DNA chains of length $l \sim 20$ nm. Assuming the correlation length $a \sim l$ we have $\frac{\langle r^2 \rangle}{a^2} \sim (\frac{\pi R}{l})^2 \simeq 10^3$. Figure 9 shows a comparison of T_{dif} and T_{dep} at constant binding free energy,

$$\frac{\Delta \bar{m}}{1 - \exp(-\bar{m})} + \ln[1 - \exp(-\bar{m})] = \text{const}. \tag{29}$$

This expression for the binding energy takes into account the entropy reduction associated with the nonergodic degrees of freedom. For a detailed discussion of this topic see Ref. [12]. Since $T_{dif} > T_{dep}$, colloidal desorption and reattachment is the dominant mechanism by which particles rearrange.

As the figure indicates, the optimal regime of fast departure is to have a large number ($\bar{m} \gtrsim 10$) of weakly bound key-lock bridges. We predict a localized regime below the crossover where particle departure is relatively fast. Just beyond the crossover there is a relative maximum in T_{dep} before it decreases at large $\bar{m}$. The increase in departure time at the onset of diffusive behavior is indicative of a regime where the system ages. In this regime the interplay of diffusion an desorption leads to longer bound state lifetimes, and an increase in the departure time.

We now turn to the question of designing a future experiment which will facilitate fast particle departure and hence
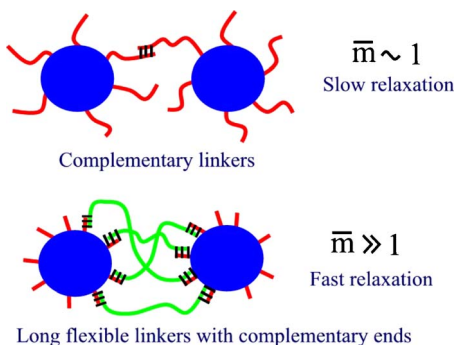
FIG. 10. (Color online) Graphical depiction comparing recent experiments with DNA-grafted colloids to a future implementation with long flexible linkers. Increasing the number of key-lock bridges between particle pairs potentially decreases the time required for crystallization.

colloidal crystallization. The essential goal is to increase the average number of key-lock bridges between particle pairs. Increasing the surface density of DNA strands alone results in the formation of a brush, which decreases the effective cross section for the interaction between complementary DNA. Instead we propose the introduction of long, flexible DNA linkers between particles with a high coverage of short ssDNA (see Fig. 10). This system has the potential to realize more key-lock bridges between particle pairs as compared to previous experiments, and therefore substantially reduce the time required for crystallization.

VII. CONCLUSION

This paper studied the dynamics of particles which interact through the reversible formation of multiple key-lock bridges. Well before the percolation threshold is reached there is a crossover from a localized regime to a diffusive regime. In the localized regime the particles remain close to their original attachment site until departing. In this regime particles are attached to finite clusters, and the system exhibits an exponential distribution of departure times. Once the radius of gyration of the cluster exceeds the characteristic radius for the particles' random walk, the finite clusters behave effectively as infinite clusters. Diffusion allows the particles to cascade into deeper energy wells, which leads to a decrease in hopping rate. The diffusion slows and the bound state lifetime increases, a phenomenon qualitatively similar to *aging* in glassy systems. In the diffusive regime we discussed the statistics for the particles' in-plane diffusion. Weak key-lock interactions give rise to a finite renormalization of the diffusion coefficient. However, as the strength of the interaction increases (larger Δ), the system exhibits anomalous, subdiffusive behavior. This situation is analogous to dispersive transport in disordered semiconductors. We then made the connection between our calculation of the departure time distribution and recent experiments with DNA-coated colloids. The findings indicate that the optimal regime for colloidal crystallization is to have a large number of weakly bound key-lock bridges. A modified experimental setup was proposed which has the potential to realize this regime of fast particle departure.

[1] P. L. Biancaniello, A. J. Kim, and J. C. Crocker, Phys. Rev. Lett. **94**, 058302 (2005).

[2] M.-P. Valignat, O. Theodoly, J. C. Crocker, W. B. Russel, and P. M. Chaikin, Proc. Natl. Acad. Sci. U.S.A. **102**, 4225 (2005).

[3] V. T. Milam, A. L. Hiddessen, J. C. Crocker, D. J. Graves, and D. A. Hammer, Langmuir **19**, 10317 (2003).

[4] N. C. Seeman, Nature (London) **421**, 427 (2003).

[5] C. A. Mirkin, R. L. Letsinger, R. C. Mucic, and J. J. Storhoff, Nature (London) **382**, 607 (1996).

[6] R. C. Mucic, J. J. Storhoff, C. A. Mirkin, and R. L. Letsinger, J. Am. Chem. Soc. **120**, 12674 (1998).

[7] N. A. Licata and A. V. Tkachenko, Phys. Rev. E **74**, 041406 (2006).

[8] S. Fan, P. R. Villeneuve, and J. D. Joannopoulos, Phys. Rev. B **54**, 11245 (1996).

[9] D. F. Sievenpiper, M. E. Sickmiller, and E. Yablonovitch, Phys. Rev. Lett. **76**, 2480 (1996).

[10] Z.-Y. Zhang and B. D. Smith, Bioconjug. Chem. **11**, 805 (2000).

[11] S. Hong, A. U. Beilinska, A. Mecke, B. Keszler, J. L. Beals, X. Shi, L. Balogh, B. G. Orr, J. R. Baker, Jr., and M. M. B. Holl, Bioconjugate Chem. **15**, 774 (2004).

[12] N. A. Licata and A. V. Tkachenko, Phys. Rev. E **74**, 041408 (2006).

[13] M. F. Sykes and M. Glenn, J. Phys. A **9**, 87 (1976).

[14] K. Kehr, K. Murthy, and H. Ambaye, Physica A **253**, 9 (1998).

[15] D. Stauffer, *Introduction to Percolation Theory* (Taylor and Francis, London, 1985).

[16] J.-P. Bouchaud, in *Soft and Fragile Matter: Nonequilibrium Dynamics, Metastability and Flow*, edited by M. E. Cates and M. R. Evans (IOP Publishing, Bristol, Philadelphia, 2000), pp. 285–304.

[17] H. Scher and E. W. Montroll, Phys. Rev. B **12**, 2455 (1975).